World Academy of Science, Engineering and Technology
International Journal of Materials and Metallurgical Engineering
Vol:10, No:4, 2016

Characterization of Metallurgical and Mechanical Properties of the Welded AISI 304L Using Pulsed and Non-Pulsed Current TIG Welding

A. A. Ugla

***Abstract*—**The present paper aims to investigate the effects of the welding process parameters and cooling state on the weld bead geometry, mechanical properties and microstructure characteristics for weldments of AISI 304L stainless steel. The welding process was carried out using TIG welding with pulsed/non-pulsed current techniques. The cooling state was introduced as an input parameter to investigate the main effects on the structure morphology and thereby the mechanical property. This paper clarifies microstructure-mechanical property relationship of the welded specimens. In this work, the selected pulse frequency levels were 5-500 Hz in order to study the effect of low and high frequencies on the weldment characteristics using filler metal of ER 308LSi. The key findings of this work clarified that the pulse frequency has a significant effect on the breaking of the dendrite arms during the welding process and so strongly influences on the tensile strength and microhardness. The cooling state also significantly affects on the microstructure texture and thereby, the mechanical properties. The most important factor affects the bead geometry and aspect ratio is the travel speed and pulse frequency.

***Keywords*—**Microstructure, mechanical properties, pulse frequency, high pulse frequency, austenitic stainless steel, TIG welding.

I. Introduction

THE austenitic stainless steels (ASS) are probably the most commonly used material of all the stainless steels especially the 300 series. AISI 304L is an important grade of the ASS, which is commonly used in many of important industries such as containers of transporting chemicals, oil refinery, nuclear reactor tanks, dairy industries, and textile industries [1]. Tungsten inert gas (TIG) welding is the most widely used process for joining the stainless steel components [2]. It is very suitable for thin sheets due to its easier applicability, flexibility, and better economy [3]. The improving in the weld quality depends on the improvement in process parameters which requires the use of improved welding techniques and materials. Pulsed current TIG welding (PCTW) is a variation of continuous current TIG welding (CCTW) where involves cycling the welding current at a given regular frequency from a high level to low level [4]. In PCTW process, the peak current (I_p) is selected to melt the filler and base metal and to generate adequate penetration, whereas the base current (I_b) is set at a level sufficient to maintain a stable arc [5]. By contrast, in CCTW, the heat required to melt the filler and base metals is supplied only during I_p pulses allowing the heat to dissipate into the base material [6]. PCTW has various good aspects over CCTW process, such as arc stability, reducing the amount of heat input, and reducing the residual stresses of stainless steel welded parts [7], [8]. Ramkumar et al. [9] used the pulsed and conventional TIG welding to study the weldability of AISI 904L stainless steel. They demonstrated that the PCTW generally offers better tensile properties as compared to CCTW weldments. Prasad et al. [10] used pulsed current in micro plasma arc welding process to study the quality of different types of stainless steels. They concluded that the AISI 304L achieved better quality characteristics compared to AISI 316L, AISI 316Ti, and AISI 321. Dinesh Kumar et al. [11] used Taguchi method to analyze and optimize the process parameters for pulsed TIG welding process of AISI 304L stainless steels. They showed that travel speed and current are the most important parameters which affect the response variables.

From the literature review, it was observed that there is a huge need for improving the quality of the ASS sheet weldments, which are used for various applications such as pressure vessels, automobile and aerospace industries. It seems worthwhile to select the most suitable welding parametric combination that would be able to create microstructural changes and weld bead characteristics and thereby improving the mechanical performance weld quality. The present paper highlights an experimental comparative study carried out to describe in detail the effects of pulse frequency and continuous water cooling system on the weld area (HAZ and bead width), depth of penetration and finding the optimal aspect ratios. Furthermore, microstructural aspects of the HAZ and weld metal and mechanical properties such as tensile strength and Vickers's micro-hardness of TIG weldments using AISI 304L ASS were investigated and correlated to the effects of process parameters on the microstructure of the weldments of CCTW and PCTW in low and high frequencies.

II. Experimental Procedure

A. Material and Welding Procedure

In this work, a 3.8 mm thick of AISI 304L stainless steel sheets have been welded by TIG technique. The filler metal selected for welding was ER 308LSi stainless steel solid wire

A. A. Ugla, Assistant Professor, is with the Department of Mechanical Engineering, College of Engineering, University of Thi-Qar, Al-Nasiriyah, Iraq (phone: +9647801324058; fax: +903423601104; e-mail: adnanugla76@gmail.com).

with a diameter of 0.8 mm. Suggested shielding gas was argon with 99.90% purity with 12 l/min. 304L stainless steel plate and the filler metal were chemically analyzed, and the results of the analysis were listed in Table I. Plates were cut using power hacksaw cutting machine. For bead on plate experiments, required plate dimensions were 100 mm x 200 mm whereas for square butt joint configuration required plate dimensions were 100 mm x 50 mm. Prepared plates were joined by CCTIG and PCTIG processes using modern TIG welding machine, which can operate in different modes such as conventional TIG welding and pulsed current TIG welding. Prepared specimens were joined with/without filler metal and with/without using a cooling system. Travel speed and arc length were controlled using CNC machine, whereas wire feed rate controlled using external wire feed machine. In the case of using the cooling system, 304L plates were placed on a copper backing plate as shown in Fig. 1. The copper backing plate contains internal passages, which were machined by drilling the plate to produce water passages in a similar way to the heat exchanger. The water interred to the passages with temperature about 20 °C to increase the cooling rate of the molten metal. The temperature was measured by placing a thermocouple near the fusion line of the welding (see Fig. 1). Type K thermocouple is the most suitable one for measuring the temperature during the welding process [12]. The temperature readings were measured using an industrial data logger, which records the temperature at an interval of one second. The pulsed current mode used in this welding machine is shown in Fig. 2. A number of trial runs were carried out in order to fix the process parameters limits and to produce samples with an adequate fusion of the base metal with filler and so resulting into sound quality welded joints. Some of the process parameters were kept as constant during all experiments such as welding current of 175 A, peak time of 50%, background current of 87.5 A, arc length of 4 mm, stick out of 15 mm, and the angle enclosed between the feeding wire and surface of the plates (feed angle) was kept at °40. In this study, four process parameters were selected for investigating the effects of process parameters on bead geometry and mechanical performance. The range of each process parameter levels was selected based on trial welds and process parameters such as travel speed (TS), wire feed speed (WFS), pulse frequency (F), and introducing the cooling state (Cs) as a new factor. Thus, the sets of process parameters used for investigating the effects on the aspect ratio (AR = bead width/depth of penetration), microstructure characteristics and mechanical properties are summarized in Table II.

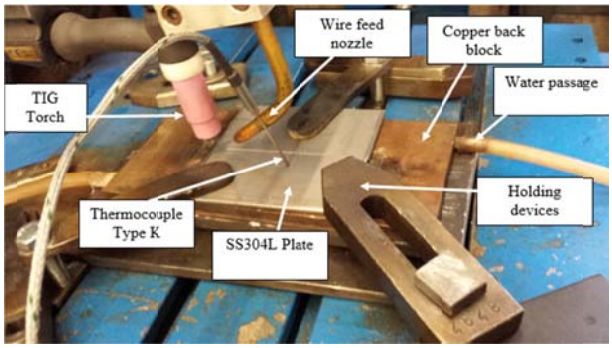

Fig. 1 TIG welding experimental setup

TABLE I
THE CHEMICAL COMPOSITION OF THE BASE AND THE FILLER MATERIALS (IN WT. %)

Element	%C	%Si	%Mn	%S	%P	%Mo	%Ni	%Cr	% Fe	Others
SS304 actual composition	0.015	0.528	1.011	0.0107	0.02	0.053	8.202	18.164	Rem.	V=0.10, Cu=0.031, Ti =0.01
ER308LSi as deposited composition	0.018	0.56	1.358	0.0331	0.033	0.115	9.412	19.557	Rem.	Co=0.941; Cu= 0.181, Ti=0.057

TABLE II
WELDING CONDITIONS USED FOR PREPARING TESTS SPECIMENS OF BUTT JOINT WELDMENTS AND RESPONSES

Exp No.	Welding process	Input factors					Response signs			
		Cs	TS (mm/s)	WFS (m/min)	Frequency F (Hz)	Aspect ratio (W/P)	S/N ratio	Peak temperature °C	Cooling rate °C/sec	Heat input Hi J/mm
1	CC TW	*0	1	0	0	4.47	-13	1046.45	7.12	1815.6
2	CC TW	**1	3	2	0	5.55	-14.9	1044	29	605.2
3	LF-PCTW	**1	2	0	5	2.83	-9.03	829	24	681
4	LF-PCTW	*0	3	4	5	7.33	-17.3	1028	13.23	454
5	HF-PCTW	**1	1	4	500	2.6	-8.3	919	13.6	1361.7
6	HF-PCTW	*0	2	2	500	3.29	-10.3	986.5	8	681

*Without cooling system; ** With continuous water cooling system

B. Weld Bead/Aspect Ratio Characteristics

The weld bead profiles of all specimens were measured carefully and the observed values for bead width and depth of penetration were used to calculate the AR and corresponding S/N ratios as summarized in Table II. The term "signal" represents the desirable mean value, and the "noise" represents the undesirable value. Hence, the S/N ratio represents the amount of variation. S/N is the performance characteristics having three types such as (1) higher the better, (2) lower the better, and (3) nominal the better. In the current work, the weld bead characteristics such as depth of the penetration and bead width of the tested weld specimens were identified as the response. The depth of penetration is considered as required sign and bead width is considered as an undesirable sign, therefore, the aspect ratio (W/P) is considered as smaller the better (SB) is used for minimizing the aspect ratio of the welded parts. The smaller the better performance is expressed

$$S/NSB= -10 \log \{(y12 + y22 + y32 \ldots yn2)/n\} \quad (1)$$

where n is the number of repetition of output response in the same trial and y is the response.

C. Metallurgical and Mechanical Characteristics

The microstructure evolution in the CCSMD and PCSMD processes was extensively investigated in this study for understanding the difference in the morphology and microstructure in both processes. Optical microscopy was used to obtain the microphotographs. Cross-section specimens were prepared for metallographic tests using the standard procedures reported in the literature [13]. All specimens were electro-etched using 10gr oxalic acid with 100 ml distilled water at 9 V for 30-60 S.

Transverse tensile tests were carried out on the subsize sheet specimens prepared according to ASTM: E8/8M standard [14] with a gauge length of 25 mm, and a cross-section of 6.25x3.8 mm^2 (see Fig. 3). Tests were performed using a testing machine with a displacement rate of 1 $mm.min^{-1}$. Three experiments were performed and averaged for assessing the ultimate tensile strength (UTS) of the weldments. Microhardness studies were carried out on the cross-section of the weldments. The measurements were taken at the center of weld metal using Vickers's microhardness testing machine. A standard test load 300 gr for a dwell period of 15 seconds was used with regular interval distance of 0.5 mm.

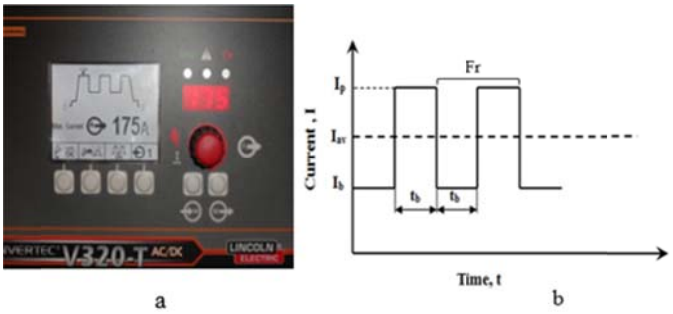

Fig. 2 (a) Welding machine screen when it is setup on the pulsed current state and (b) Schematic diagram of a standard pulse current-time waveform in the present PC-TW process; I_p: peak Current (5-250 A); I_b: background current (5-95% of the I_p); t_p: peak current duration (ms); t_b: base current duration (ms); LF: low frequency (0.2-100 Hz); HF: high frequency (500-2500 Hz); On-line pulse (5-95 %)

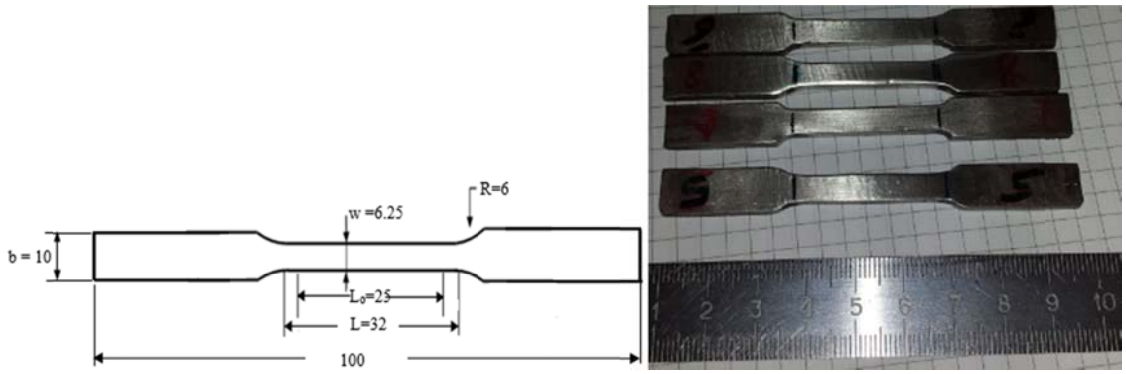

Fig. 3 Standard tensile specimens (a) Sub-size specimen; (b) Real tension test specimens prepared according to ASTM E8/8M standard [14]

III. Results and Discussions

A. S/N Ratios of Aspect Ratio Analysis and Main Effects Plot

The heat affected zone (HAZ) decreases the strength of the welded parts and reduce the efficiency of the joints due to the metallurgical changes at this region such as grain growth. Most of the tensile test specimens are failed at HAZ. Therefore, HAZ should be reduced to a minimum as can as possible by reducing the cooling time (using the cooling system) or using pulse current welding method. Fig. 4 presents the weld area (HAZ + bead width) of the welded specimens using conventional and PCTW techniques. It is obvious that with high frequency (exp. 6) the welded area significantly reduces and hence weldment efficiency improves.

Various aspect ratios of bead width and depth of penetration were calculated experimentally for all experiments as listed in Table II. The main effects plots for the S/N ratios are shown in Fig. 5, which shows that the S/N values increase with increasing the cooling rate, F and also TS from 1 mm/s to 2 mm/s. On another hand, S/N values decrease with increasing the WFS, and with increasing TS from 2 mm/s to 3 mm/s. The optimal process parameters have been established by analyzing response curves of S/N ratio as shown in Table III. It is concluded that the TS of 2 mm/s, no filler wire, the frequency of 500 Hz and continuous water Cs) gives the optimal aspect ratio.

B. Microstructure Characteristics

From the aforementioned results in Table II, the heating and cooling curves for all experiments are shown in Fig. 6. The peak temperature values are listed in Table II. The cooling rate was calculated for temperature drop from peak to 300 °C.

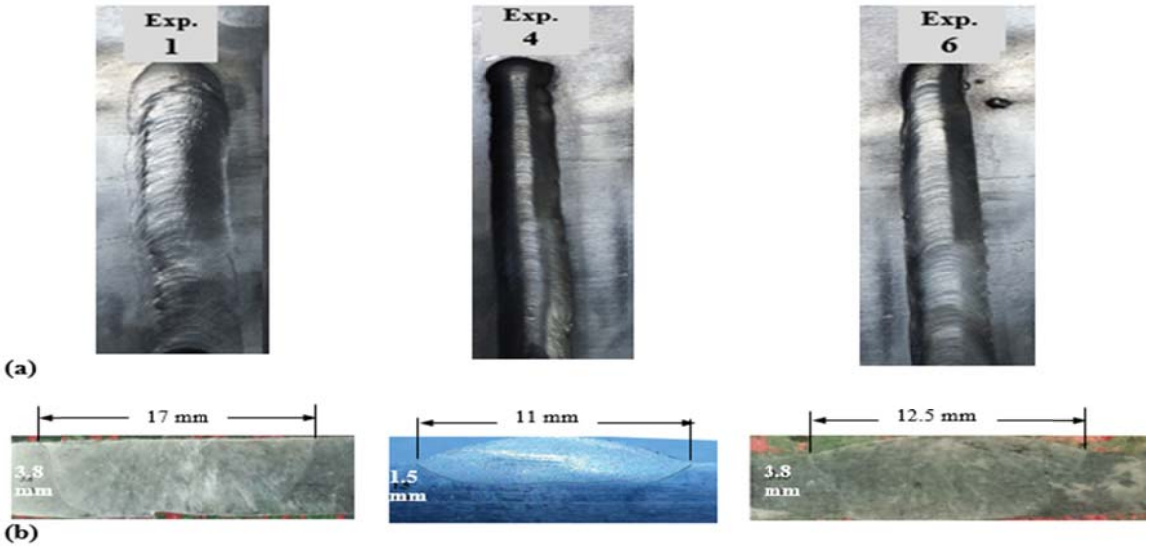

Fig. 4 Macrographs of AISI 304L joints illustrate (a) Top view of the bead profile and (b) Cross-section views of the etched specimens showing the amounts of bead width and depth of penetration

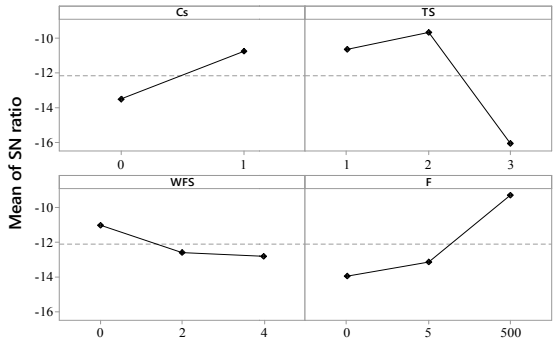

Fig. 5 Effects of main factors on S/N ratio of the aspect ratio of the weld bead geometry

TABLE III
OPTIMIZED PARAMETERS FOR LOWER ASPECT RATIO (AR)

S. No	Factor	Level	Value	Rank	Percent contribution
1	Cs	2	Continuous water cooling system	3	19 %
2	TS	2	2 mm/s	1	47 %
3	WFS	1	No filler wire	4	0.3 %
4	F	3	500 Hz	2	25 %

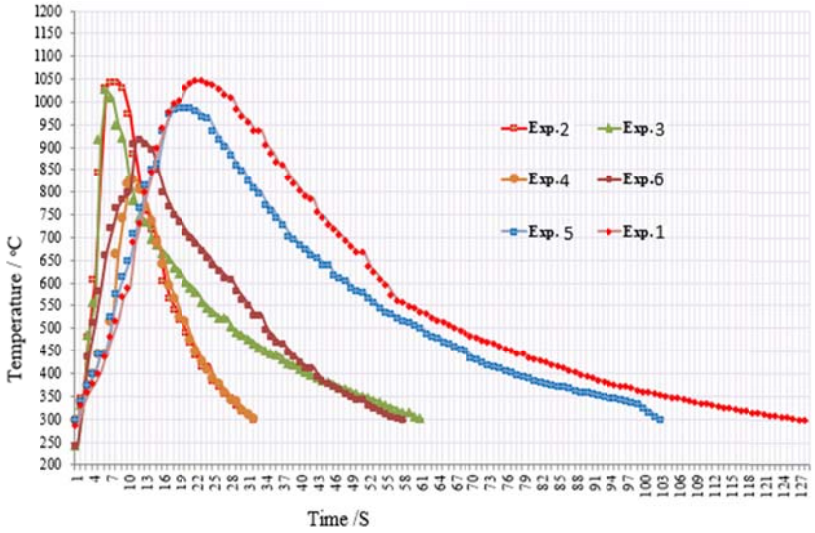

Fig. 6 The heating and cooling curves

From the microstructure results, it is clear that two different kinds of delta-ferrite (δ-ferrite), namely lathy and skeletal δ-ferrite are formed in the austenitic matrix. Fig. 7 shows the variation of δ-ferrite morphology in weld zone with Cs and other parameters in CCTW process of experiments 1 and 2. Experiment 1 shows the microstructure of a specimen

prepared without using the copper strip and without adding filler metal, whereas experiment 2 shows the effects of using the continuous water cooling system and with adding filler metal. Fig. 7 (a) depicts greater skeletal and vermicular δ-ferrite with high grain size, and Fig. 7 (b) reveals that the grain size generally was finer and a higher concentration of total δ-ferrite content compared to experiment 1 (Fig. 7 (a)).

Figs. 8 (a)-(c) show the base metal (BM), HAZ, fusion zone (FZ), and weld metal (WM) of CCTW, low-frequency LF-PCTW, and high-frequency HF-PCTW weldments respectively. It is obvious that all weldments consist of a columnar dendritic structure with a vertical fusion line. It indicates that growth takes places along the direction of the maximum temperature gradient. From Fig. 8 (c), it can be seen that the high cooling rate associated with PCTW process results in a narrow HAZ as comparing to CCTW process (Fig. 8 (a)). Figs. 8 (d)-(f) give the microstructures of the interface between HAZ and FZ for CCTW, LF-PCTW, and HF-PCTW weldments without using water Cs (Cs =0). It is noted that the grains in HAZ near fusion boundary are coarse. In FZ, because the temperature gradient is high, the crystallization rate is small (low grain growth rate). For CCTW weldment, the low cooling rate leads to grain growth at the HAZ (Fig. 8 (d)) whereas for the PCTW weldment, F has a significant effect on the solidified weld pool and so less grain growth is apparent in the HAZ than in BM region (see Fig. 8 (f)). Figs. 8 (g)-(i) show the microstructure of the central zone of WM for the CCTW, LF-PCTW, and HE-PCTW respectively. Fig. 8 (i) shows that the pulsed current with high frequency tends to produce a smaller grain size and a more refined solidification than the continuous current welding method (Fig. 8 (g)). This microstructural difference will be reflected in the different mechanical behavior of the three weldment types.

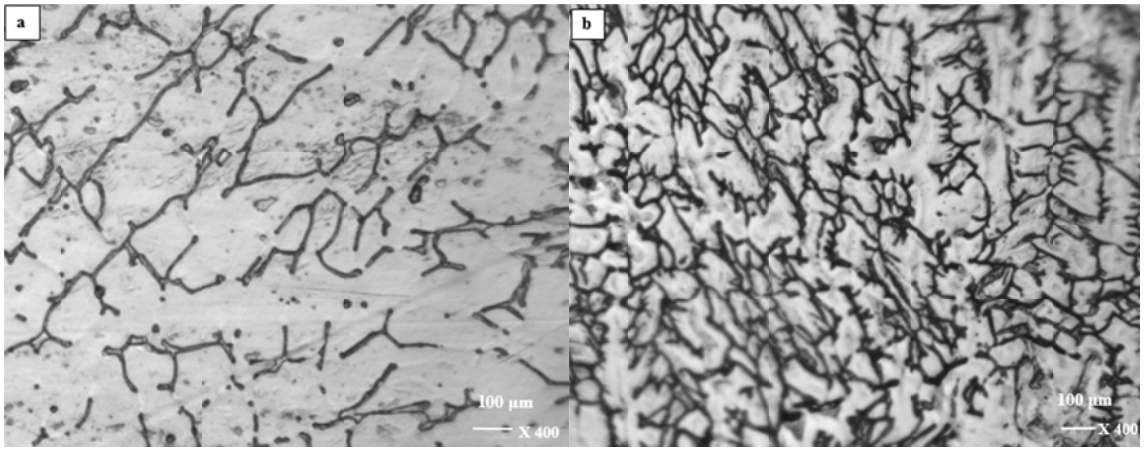

Fig. 7 CCTW (a) exp. 1 (TS 1mm/s, WFS 0, no cooling system), and (b) exp. 2 (TS 3 mm/s, WFS 4 m/min, continuous water cooling system) Existing of long dendrites arms and continuous network of residual ferrite

The changes in microstructure associated with the amount of heat input to weld pool during the deposition process according to (2) [15]:

$$\text{Hi}\left(\frac{\text{J}}{\text{mm}}\right) = \eta \text{I}\frac{\text{Vav}}{\text{TS}} \quad (2)$$

where Hi is the heat input per unit length; η is arc efficiency (assumed to be 0.83) for TIG welding [12], V_{av}: the average of the instantaneous arc voltage.

In PCSMD process, the heat input can be calculated using (2) but here the welding current is I_{av} as shown in (3) [16], [17] and the average peak current for pulsed current can be calculated using (4) [18]:

$$\text{Hi}\left(\frac{\text{J}}{\text{mm}}\right) = \eta \text{Iav}\frac{\text{Vav}}{\text{TS}} \quad (3)$$

$$\text{I}_{\text{av}}.\,(\text{A}) = \frac{\text{Iptp+Ib tb}}{\text{tp+tb}} \quad (4)$$

where I_{av} the average current for pulse current TIG welding, t_p is the peak time (s) and t_b is the base current duration (s), I_p is the peak current and I_b is the base current.

The amount of δ-ferrite exists in WM depends on several factors, the most significant factors are chemical composition of the filler and BM, welding procedure, and the amount of heat input to the melting pool during the welding process [19]. Furthermore, the process of rapid solidification with a high-temperature gradient, it is beneficial to obtain fine microstructure. Low heat input to the weld zone may result from high TS, using the continuous cooling system, and/or using high F. High frequency leads to break the dendritic arms of the ASS and produces uniform structure (see Fig. 8 (i)). Mourad et al. [20] demonstrated that residual ferrite is strongly influenced by the heat input. At high cooling rates, which result from the pulsed current process, high TS, or continuous water cooling system the transformation of δ-ferrite to austenite is suppressed and higher residual ferrite content in the welding metal is expected as shown in Figs. 8 (h), (i). Fig. 9 describes the effects of high-frequency (500 Hz) of the pulsed current on columnar grains as comparing to conventional current process. It is obvious that F significantly affects the dendrites arms of the solidified structure at WM and hence it influences the tensile properties welded parts.

C. Mechanical Test Results

The tensile test results are summarized in Fig. 10. It is obvious that the highest UTS was achieved at high frequency (500 Hz) and continuous water cooling conditions (experiment 5), also high UTS was obtained at low frequency (5Hz) and continuous water cooling state (experiment 3). UTS is also improved using the continuous water cooling system in the CCTW process (experiment 2). From Fig. 10, the lowest UTS occurred in the specimens were prepared using a set of process parameters in experiments 4 (see Table II). The deterioration of UTS was attributed to insufficient heat input which is necessary for melting the filler and base metals during the welding process and so leads to incomplete fusion as shown in Fig. 4. Fig. 11 shows that the frequency is the most significant factor influences the microhardness since it significantly affects the grain size through breaking the dendrite arms as well as the amount of δ-ferrite is relatively higher (see Fig. 8 (i)). From the Fig. 11, it is obvious that the cooling condition also significantly effects on the microhardness, since it increases the cooling rate and creates a fine structure with high residual δ-ferrite content (see Fig. 7), which leads to increase the hardness of the weldments. The highest tensile strength achieved during this research is 765.8 MPa at a frequency of 500 Hz and using the continuous water cooling system. While highest hardness obtained is 308 HV at a frequency of 500 Hz and using the continuous water cooling system.

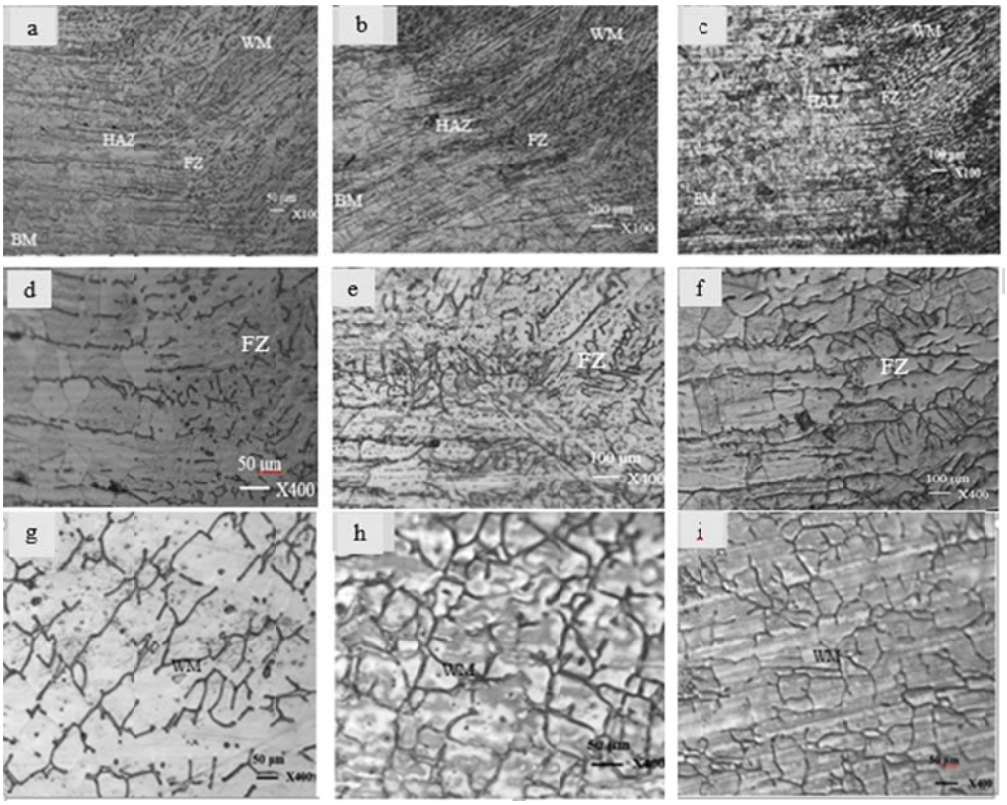

Fig. 8 Optical microstructures of (a) CCTW; (b) LF-PCTW; (c) HF-PCTW; (d) WM of CCTW; (e) WM of LF-PCTW; (f) WM of HF-PCTW

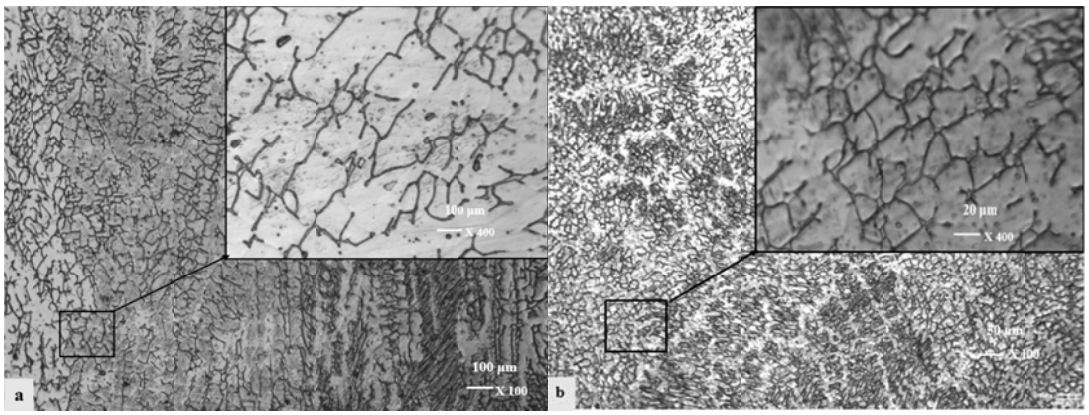

Fig. 9 Micrographs of the effects of frequency on the dendritic arms (a) continuous current (experiment 1) and (b) pulsed current (experiment 5)

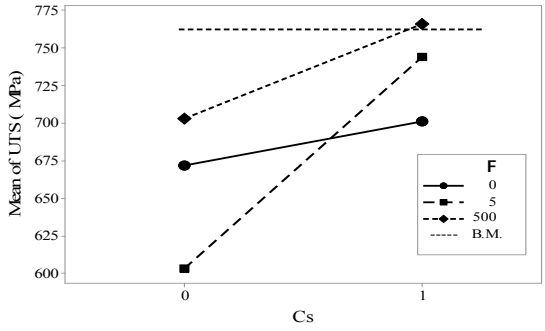

Fig. 10 UTS versus F and Cs comparison to BM

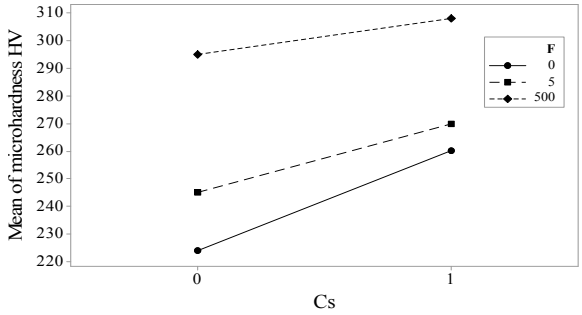

Fig. 11 The effects of F and Cs on the microhardness (HV)

IV. Conclusions

This paper presented the optimization of welding process parameters using 3.8 mm sheets of AISI 304L stainless steel material through experimental study for non-pulsed & pulsed current TIG welding. The main outcomes of this work have been deduced as concluding summary as follows:

1. The results show that TS is the most significant factor influences the aspect ratio with contribution percent of 47% followed by F of the contribution of 25%, then Cs with contribution percent of 19% and no effect of wire feeding rate.
2. Optimal aspect ratio can be achieved through using HF-PCTW process with the following optimal values of welding conditions: TS 2 mm/s, WFS 0 m/min, F 500 Hz, and continuous water cooling rate system. F significantly affects by reducing the width of the weld area and hence reducing the HAZ.
3. HF-PCTW significantly influences on the morphology of the welded parts and hence improves the mechanical properties. Since it significantly affects the grain size through breaking the dendrite arms as well as the amount of δ-ferrite is relatively higher. Whereas, Cs factor also affects the tensile strength, since it creates a fine structure with high residual δ-ferrite content which leads to improving the properties of the weldments.
4. The highest tensile strength achieved during this study is 766 MPa achieved at a frequency of 500 Hz and using the continuous water cooling system. Thus, the HF-PCTW can be used to fabricate joints with a tensile strength superior to that of CCTW process. The highest hardness reached to 308 HV in weld zone, also achieved at high frequency and continuous water cooling system.
5. From the microstructure analysis, there is no evidence of any sensitization of the welded parts can be seen for all weldments (CCTW and PCTW) also no other defects can be observed.

References

[1] K. D. Ramkumar, A. Choudhary, S. Aggarwal, and A. Srivastava, "A review on welding of AISI 304L austenitic stainless steel",*J. Manuf. Sci. Prod*. Vol. 14, N. 1, 2014, pp 1-11.

[2] K. B. Hamjah, "*Optimization of new semi-automatic TIG welding process for surface quality through Taguchi method*," PhD Thesis, University of Tun Hussein Onn, Malaysia, 2014.

[3] J. Mao, W. LÜ, L. Wang, D. Zhang, J. Qin, "Microstructure and mechanical properties of GTA weldments of titanium matrix composites prepared with or without current pulsing," *J. Trans. Nonferrous Met. Soc. China*, vol. 24, 2014, pp. 1393-1399.

[4] A. Namjou, R. Dehmolaei, A. Sharafi, "A Comparative study," in Magnetism, vol. III, on direct pulsed current gas tungsten arc welding of 25Cr-35Ni heat resistant steel," *Int. J. Natu. Eng. Sci*., Vol. 8, N.11, 2014, pp. 22-28.

[5] M. Yousefieh, M. Shamanian, A. Saatchi, "Optimization of the pulsed current gas tungsten arc welding (PCGTAW) parameters for corrosion resistance of super duplex stainless steel (UNSS322760)welds using the Taguchi method," *J. Alloy Compd*, vol 209, 2011, pp. 782-790.

[6] B. Balasubramanian, V. Jayabalan, V. Balasubramanian, "Optimizing the pulsed current gas tungsten arc welding parameters," *J. Mater. Sci. Technol.*, Vol. 22, N. 6, 2006, pp. 821-825.

[7] K. Pal, S.K. Pal, "Effect of pulse parameters on weld quality in pulsed gas metal welding: A review", *J. Mater. Eng. Perf.* Vol. 20, N.6, 2011, pp. 918-931.

[8] K.H Tseng, C.P. Chou, "The effect of pulsed GTA welding on the residual stress of a stainless steel weldment", *J. mater. Proc. Technol*. Vol. 123, N. 3, 2002, pp. 346-353.

[9] K. D. Ramkumar, A. Choudhary, S. Aggarwal, and A. Srivastava, "Characterization of microstructure and mechanical properties of continuous and pulsed current gas tungsten arc welded super austenitic stainless steel," *J. Mater. Res.* Vol. 30 No. 10, 2015, pp. 1727-1746.

[10] K. S. Prasad, C. S. Rao, and D.N. Rao, "An investigation on weld quality characteristics of pulsed current micro plasma arc welded austenitic stainless steels," *Int. J. Eng. Sci. Technol*. Vol. 4, No. 2, 2012, pp.159-168.

[11] R. Dinesh Kumar, S. Elangovan, and N. Siva Shanmugam, "Parametric optimization of pulsed-TIG welding process in butt joining of 304L austenitic stainless steel sheets," *Int. J. Res. Eng. Technol.* Vol. 3, No. 11, 2014, pp. 213-219.

[12] C. Sadek, A. Alfaro, K.S. Chawla, J. Norrosh "Computer-based data acquisition for welding research and production" *J. Mater. Proc. Technol.*, Vol. 53, 1995, pp. 1-13.

[13] Metals Handbook, (1973) Metallographic, structures, and phase diagrams. 8th Edition, American Society for Metals, Metal Park, Ohio 44073 USA.

[14] ASTM International. Standard test methods for tension testing of metallic materials (metric). Standard E8/E8M-09, *ASTM International, W. Conshohocken*, Pa, 2011.

[15] S. Kou (2003) Welding Metallurgy.2nd Edition, John Wiley &SONS, INC.

[16] P.K. Griridharan, N. Murugan, "Optimization of pulsed GTA welding process parameters for the welding of AISI 304Lstainless steel sheets", *Int. J Adv. Manu Technol*., Vol.40, 2009, pp. 478-489. doi: 10.1007/s00170-008-1373-0.

[17] M. Arivarasu, K. Devendranath, N. Ramkumar Arivazhagan "Comparative studies of high and low frequency pulsing on the aspect ratio of weld bead in gas tungsten arc welded AISI 304L plates", *Procedia Engineering* Vol.97, 2014, pp. 871-880.

[18] E. Farahani, M. Shamanian, F. Ashrafizadeh "A comparative study on direct and pulsed current gas tungsten arc welding of alloy 617", *Int J on Manuf and Material Science*, Vol. 2, 2012, pp. 1-6. doi: 01IJMMMS.0201.41.

[19] A. Eghlimi, M. Shamanian, and K. Raeissi, "Dilution and ferrite number prediction in pulsed current cladding of super-duplex stainless steel using RSM," *J. Mater. Eng. Per*., vol. 22, No. 12, 2013, pp. 3657-3664.
[20] A.H.I Mourad, A. Khourshid, and T. Sharif, " Gas tungsten arc and laser beam welding processes effects on duplex stainless steel 2205 properties," *Mater. Sci. Eng. A*, vol. 549, 2012, PP. 105-113.